# Quantitative assessment of a second-generation cryoballoon ablation catheter with new cooling technology—a perspective on potential implications on outcome

**Sven Knecht · Michael Kühne · Stefan Osswald · Christian Sticherling**

**Abstract**

*Purpose* The purpose of this study was to assess the differences in cooling behavior between the first-generation cryoballoon (CB-1G) and the second-generation cryoballoon (CB-2G) quantitatively to understand the freezing capabilities and to benefit from the improved efficacy of the CB-2G in patients with atrial fibrillation.

*Methods* We analyzed quantitatively the ice formation of the CB-1G and CB-2G catheters *in vitro* in a 37 °C warm water bath during freezing for 60, 120, 180, 240, and 300 s, respectively.

*Results* The mean-covered surface area and the relative coverage of the ice spots on the CB-2G were significantly different from the spots on the CB-1G for the 28-mm CBs but not for the 23-mm CBs. Whereas for the CB-1G, the ice formation was discontiguous with four isolated ice spots; the CB-2G showed a contiguous ice cap covering the entire distal part including the pole of the balloon. No homogeneous cooling behavior could be observed at the equatorial level with both catheters. Temporal differences on the ice formation could be observed for the 28-mm CB-2G but not for the 23-mm CB-2G.

*Conclusion* The new-generation CB-2G showed more powerful and homogeneous cooling behavior, especially for the 28-mm CB. Whether this translates into higher long-term success rates is currently unknown. The impact of the more effective cooling and the longer dissolving duration of the ice cap of the new-generation CB-2G on procedural safety needs to be investigated.

**Keywords** Cryoballoon technology · Pulmonary vein isolation · Atrial fibrillation

## 1 Introduction

Cryoballoon (CB) ablation catheters are increasingly used as an alternative to point-by-point ablation using radiofrequency energy for pulmonary vein isolation (PVI) for the treatment of atrial fibrillation. Despite being engineered as a simple device to create a complete circumferential lesion around the pulmonary veins with only a limited number of applications, the first-generation cryoballoon (Artic Front, Medtronic, MN, USA) showed heterogeneous cooling behavior resulting in nonuniform temperature distribution on the CB surface [1]. Several anatomical predictors for the acute and mid-term failure of PVI have been identified that can at least in part be explained by this cooling pattern. Recently, a second-generation CB (Arctic Front Advance) has been approved for PVI in the USA, Canada, and Europe. The constructional changes of the second-generation CB aim to address this limitation and to improve acute PVI success rates, success rates in more challenging anatomical variants, and potentially the permanency of PVI after CB ablation [2]. The impact of these changes on clinical outcome and safety is currently unclear. First results from two animal studies and one human study demonstrated improved acute efficacy [3–5], but critical comments regarding the current recommendations for the use of the cryoballoon have been published [6]. To be able to benefit from its improved efficacy without impairing the safety of the procedure, the freezing capabilities of the CB

Sven Knecht and Michael Kühne contributed equally to this manuscript

S. Knecht (✉) · M. Kühne · S. Osswald · C. Sticherling
Cardiology/Electrophysiology, University Hospital Basel,
Petersgraben 4, 4031 Basel, Switzerland
e-mail: knechts@uhbs.ch

have to be understood. Currently, however, only qualitative descriptions and sketches of the potential cooling behavior of this new device exist [5, 7].

The purpose of this study was to assess the differences in cooling behavior between the first-generation cryoballoon (CB-1G) and the second-generation cryoballoon (CB-2G) quantitatively.

## 2 Methods

Freezing cycles using the first generation (CB-1G) and second generation (CB-2G) were performed in a static 37 °C warm water bath showing an almost identical freezing parameter than blood. To compare the freezing behavior of the commonly used application duration of 300 s for the CB-1G and 240 s for the CB-2G catheters, we performed three freezes for each of the three 23-mm CB and of the three 28-mm CB of both generations. To investigate the time dependency of the cooling behavior of the CB-2G, we performed freezing cycles of 60, 120, 180, and 240 s for three 23-mm CBs and three 28-mm CBs, respectively.

For better visualization of the ice cap for subsequent quantification, blue dye was added to the water. After completing the freezing cycle, the CB was removed from the water bath, photographed immediately in two views, and re-submerged into the water bath to measure the time until deflation. The pictures of the CB catheters with the resulting ice caps were analyzed using a visualization application (ParaView 3.12.0) and quantified with the implemented ruler. Maximal thickness and the diameter of the ice caps of the CB-1G and the thickness of the ice cap at the pole and the minimal and maximal ice coverage of the CB-2G were measured (Fig. 1). Absolute and relative coverage of the ice cap were calculated for the entire balloon surface. The maximum diameter of a pulmonary vein than can theoretically be isolated based on the ice formation was measured for the above-described data (Fig. 2). For *in vivo* comparison, data from 53 freezing cycles using an arbitrary sample of consecutive patients, 3

treated with the CB-1G and 3 treated with the CB-2G, was analyzed.

## 3 Statistical analysis

Continuous variables are presented as mean plus or minus standard deviation (±SD). Comparisons were made using Student's *t* test or one-way ANOVA using Tukey post hoc tests ($p = 0.05$). A two-tailed *p* value <0.05 was considered statistically significant. Analysis was performed using SPSS 21.0 (SPSS Inc., Chicago, USA).

## 4 Results

### 4.1 *In vitro* behavior of CB-1G

For the 23- and 28-mm CB-1G, the mean thickness and mean-covered surface area of the ice spots were $2.8 \pm 0.4$ and $3.2 \pm 0.4$ mm and $740 \pm 153$ and $430 \pm 182$ mm$^2$, respectively (Table 1). This resulted in a mean relative coverage of the entire surface of $52 \pm 10$ and $17 \pm 7$ %, respectively, after a freezing duration of 300 s. In all tests, the ice distribution on the surface was not homogenous with four separated ice spots as shown in the example in Fig. 1. In only one of the 23-mm CB, ice formation could be observed at the pole of the CB. Minimal temperature of the freezes performed *in vitro* was $-63 \pm 2$ and $-47 \pm 2$ °C for the 23- and 28-mm CB, respectively. Mean time till deflation of the 23- and 28-mm CB at 20 °C was $76 \pm 42$ and $44 \pm 15$ s, respectively.

### 4.2 *In vitro* behavior of the CB-2G

For a freezing duration of 240 s, the CB-2G showed a complete ice cap covering the distal part of the balloon in 100 % of the tests for both CB diameters. The minimal temperature of the freezing cycles for the 23- and 28-mm CB in the water bath was $-52 \pm 2$ and $-47 \pm 2$ °C, respectively, with a mean
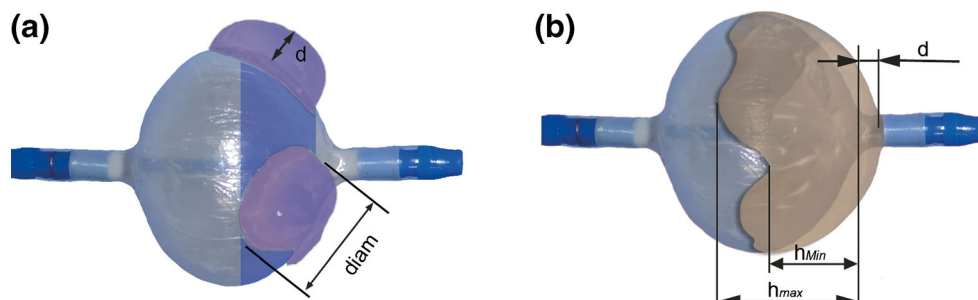


**Fig. 1** Measurements performed on the ice caps of a first-generation (**a**) (CB-1G) 28-mm CB and a second-generation (**b**) (CB-2G) 28-mm CB. The *blue area* in **a** represents the optimally cooled area assuming rotation

of the balloon between subsequent freezes. *diam* diameter of the ice spot, *h$_{min}$* minimal ice coverage, *h$_{max}$* maximal ice coverage
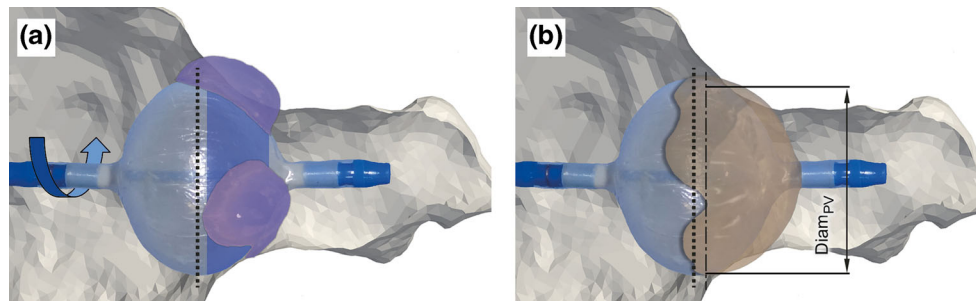
**Fig. 2** Cryoballoon with the ice caps visualized in a pulmonary vein. The equators of the cryoballoons are highlighted by the *dashed line*. **a** The *blue area* represents the critical balloon surface that can be covered by rotation of the CB-1G. **b** Measurement of the maximal diameter of the PV that can be treated with CB-2G without rotation, determined by $h_{min}$

thickness of the ice cap at the pole of 2.9±0.6 and 3.0± 0.6 mm, respectively (Table 1). This thickness was comparable to the CB-1G (Table 1). The area of the homogeneously covered ice cap of the 23-mm CB-2G was similar to the one of the 23-mm CB-1G, resulting in a mean relative coverage of 42 ±4 and 52±10 %, respectively ($p=0.119$). For the 28-mm CB, the area of the homogeneously covered ice cap of the CB-2G was significantly larger ($p=0.016$) compared to the area of the CB-1G resulting in a mean relative coverage of 27±8 and 17± 7 % ($p=0.007$), respectively.

Neither for the 23-mm CB-2G nor for the 28-mm CB-2G, a complete ice cap could be observed at the equatorial level of the CB-2G, reflected by a minimal length of the ice cap ($h_{min}$) of 8.1±0.6 mm (23-mm CB) and 7.7±2.2 mm (28-mm CB), which is smaller than half the balloon size. This transfers into a maximal diameter of the CB with homogeneous cooling of 25.4±1.0 mm for the 28-mm CB-2G and of 21.8±1.1 mm for the 23-mm CB-2G (Table 1). At the level of the equator of the balloon, a typical sinusoidal pattern of the ice cap could be observed in eight of nine tests for the 23-mm CB (89 %) and in seven of nine tests for the 28-mm CB (78 %). In the three freezing cycles, an asymmetrical ice cap could be observed, most likely due to a partially occluded refrigerant nozzle.

For the four different freezing durations, the maximal thickness of the ice cap, the absolute and the relative area of the homogeneously covered ice cap, and the maximal diameter of the homogeneously cooled surface were significantly different for the 28-mm CB ($p<0.001$) but not for the 23-mm CB (Table 2). Post hoc analysis revealed that the diameter and the homogeneously covered surface area and the ice-covered surface area were not significantly different between freezes with a duration of 240 and 180 s and between 60 and 120 s for the 28-mm CB.

### 4.3 Clinical *in vivo* data

Minimal CB temperature of three consecutive patients treated with the CB-1G and the three patients treated with the CB-2G catheter (overall 27 and 26 freezing cycles, respectively) was −43±7 and −45±9 °C, respectively, and time to deflation was 27±13 and 49±19 s ($p<0.001$) (Table 3). The power to detect a difference of 15 s between the two CBs in the *in vivo* dataset with a mean duration of 27 s for the CB-1G and a SD of 20 s was 0.97.

## 5 Discussion

In April 2012, Medtronic received a Premarket Approval (PMA) from the Food and Drug Administration (FDA) for

**Table 1** Summary of the *in vitro* data after a freezing duration of 300 s for the CB-1G and 240 s for the CB-2G

| | 23-mm CB | | | 28-mm CB | | |
|---|---|---|---|---|---|---|
| | CB-1G | CB-2G | *p* value | CB-1G | CB-2G | *p* value |
| Temperature [°C] | −63±2 | −52±2 | <0.001 | −47±2 | −47±2 | 0.629 |
| Time to deflation [s] | 76±42 | 95±5 | 0.471 | 44±15 | 100±34 | <0.001 |
| Max. Thickness [mm] | 2.8±0.4 | 2.9±0.6 | 0.800 | 3.2±0.4 | 3.0±0.6 | 0.497 |
| Absolute area [mm$^2$] | 740±153 | 585±42 | 0.151 | 430±182 | 690±197 | 0.016 |
| Relative area [%] | 52±10 | 42±4 | 0.119 | 17±7 | 27±8 | 0.007 |
| Min. length $h_{min}$ [mm] | n.a. | 8.1±0.6 | n.a. | n.a. | 7.7±2.2 | n.a. |
| Max. length $h_{max}$ [mm] | n.a. | 14.1±1.9 | n.a. | n.a. | 16.5±2.1 | n.a. |
| Max. diameter [mm] | n.a. | 21.7±1.1 | n.a. | n.a. | 25.4±1.0 | n.a. |

*n.a.* not available

**Table 2** Time-dependent parameter for the 23- and 28-mm CB-2G

| Duration [s] | 23-mm CB-2G | | | 28-mm CB-2G | | |
|---|---|---|---|---|---|---|
| | Thickness [mm] | Area [mm$^2$] | Diameter [mm] | Thickness [mm] | Area [mm$^2$] | Diameter [mm] |
| 60 | 2.2±0.2 | 421±26 | 20.0±0.5 | 1.7±0.3 | 436±27 | 22.2±1.1 |
| 120 | 2.3±0.2 | 472±15 | 20.8±0.7 | 2.2±0.3 | 517±102 | 23.5±1.9 |
| 180 | 2.3±0.1 | 497±23 | 21.2±0.2 | 2.4±0.2 | 619±96 | 24.3±1.0 |
| 240 | 2.8±0.5 | 585±42 | 21.8±1.1 | 3.0±0.4 | 725±84 | 25.4±1.0 |
| p | 0.102 | 0.001 | 0.096 | <0.001 | <0.001 | <0.001 |

*Diameter* max. diameter with homogeneous ice coverage

"catheter changes to increase the uniformity of the distal balloon surface temperature (increased number of refrigerant ports on the injection tube coil, more distal position of the injection tube, increased refrigerant flow on the 28 mm balloon), to add new visual marker on the catheter shaft and to implement additional minor changes to the design and labeling" [8]. The reason for submitting the supplement (Supplement Number S015 to PMA number P 100010) was classified as "Design Change—Minor". In the present study, we quantified the effect of these constructional changes of the second-generation cryoballoon (CB-2G) compared to the first-generation cryoballoon (CB-1G) on the cooling behavior *in vitro*.

In contrast to the first-generation CB, a significantly larger ice formation with a homogeneous ice distribution pattern and consequently a longer thawing period with a prolonged time to deflation can be observed after the recommended freezing duration of 240 s with the CB-2G. Especially in the pole region of the CB-2G, there is complete coverage of the balloon surface. Therefore, homogeneous cooling can be expected *in vivo* in the entire distal one third of the CB. However, no homogeneous cooling can be observed at the equatorial level of the CB-2G, and there were three cases of atypical ice cap formation, possibly due to occlusion of the refrigerant nozzle.

The technical changes of the CB-2G resulted in significant changes of the investigated parameters compared to the CB-1G mainly for the 28-mm CB. This might be explained by the increased refrigerant flow coming along with the second generation of the 28-mm CB and the greater benefit of the doubling of the number of refrigerant jets on the approximately 50 % bigger surface area compared to the 23-mm CB. For

**Table 3** Summary of the *in vivo* data

| | CB-1G | CB-2G | P |
|---|---|---|---|
| Temperature [°C] | −43±7 | −45±9 | 0.377 |
| Time to deflation [s] | 27±13 | 49±19 | <0.001 |

*CB-1G* first-generation cryoballoon, *CB-2G* second-generation cryoballoon

the 23-mm CB of the first generation, the surface was already nicely covered by the four refrigerant jets, resulting in a similar surface area than with the eight jets of the second-generation balloon.

### 5.1 Potential clinical implications

The increase of the number of refrigerant jets from four to eight, the more distal positioning of the refrigerant injection coil, and an increase of the fluid flow to compensate for the increased injection area resulted in a homogeneously covered distal part of the CB-2G in all tests. Except for the 3 out of the 18 freezing cycles with asymmetrical freezing pattern, a typical sinusoidal pattern of the ice cap at the equatorial plane can be observed (Fig. 1). In none of the cases, a complete ice cap could be observed at the equatorial level of the CB-A.

Recently, we published anatomical predictors for PVI failure using the first-generation cryoballoon [1]. A sharp carina or a sharp ridge between the left superior pulmonary vein and the left atrial appendage was identified as a predictor for acute failure of PVI in a multivariate analysis. These obstacles may be overcome by the CB-2G. The more homogeneous cooling over the distal one third of the CB-A can be expected to result in a higher acute success rate for PVI even for small veins using the 28-mm cryoballoon and other challenging
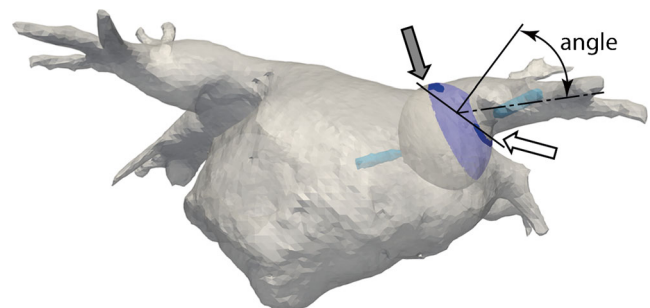


**Fig. 3** Inferior view of a left atrium with the old-generation CB visualized in the right inferior PV. The *blue area* represents the coldest area. The *arrows* indicate regions with suboptimal contact with lower cryoballoon temperature. The *white arrow* indicates the region where improvement of freezing can be expected with the second-generation CB

anatomical variations. This is reflected in the early clinical experience with the CB-A reported by Fürnkranz et al. who showed a significantly higher single-shot PVI rate of 84 % with the CB-2G compared to 51 % with the CB-1G [5]. Furthermore, the technical changes of the CB-2G may allow for successful PVI with less precise alignment of the catheter (Fig. 3). Due to a reduced and less homogeneous cooling behavior at the equator of the CB-2G, a rotation or positional change of the balloon catheter might still be needed in certain situations in order to achieve a continuous circumferential lesion. For a freezing cycle with optimal heat transfer, utilizing the homogeneously cooled distal one third of the balloon, the PV diameter should be smaller than 21 and 25 mm with an axially oriented 23- and 28-mm cryoballoon, respectively, based on the homogeneous cooling of the tip (Fig. 2). If larger veins are targeted or the orientation of the CB is not aligned with the PV axis, equatorial contact with reduced and less homogeneous cooling behavior results in suboptimal heat transfer, but this might still be sufficient to achieve isolation in a majority of PVs.

Temporal analysis of the freezing behavior revealed for the 28-mm CB-2G, a similar cooling behavior after 240 and 180 s in terms of the surface area and the maximal diameter of the CB with homogenous cooling. Consequently, by reducing the freezing duration from 240 to 180 s, no difference regarding the alignment of the catheter for optimal heat transfer might be observed, whereas for a shorter freezing duration, the CB alignment might become more important again. For the 23-mm CB-2G, these might be negligible, and the parameter primarily influencing the efficacy of the cryoballoon application is the freezing duration itself. Whether the improved cooling has as well an impact on prediction of phrenic nerve palsy [9] and other safety concerns needs further investigation.

## 6 Limitations

Freezing cycles were performed *in vitro* in a water bath with 37 °C without any surface contact to the myocardium and fluid flow which might result in absolute temperature differences and ice volumes. Our results, however, reflect the differences of the two CB generations, which can be expected to be similar under same conditions *in vivo* and *in vitro*.

## 7 Conclusions

The new-generation CB-2G showed more powerful and homogeneous cooling behavior, especially at the pole of the balloon. Whether this translates into higher long-term success rates is currently unknown. The impact of the more effective cooling and the longer dissolving duration of the ice cap of the new-generation CB-2G on procedural safety needs to be investigated.

## References

1. Knecht, S., Kühne, M., Altmann, D., Ammann, P., Schaer, B., Osswald, S., & Sticherling, C. (2013). Anatomical predictors for acute and mid-term success of cryoballoon ablation of atrial fibrillation using the 28mm balloon. *Journal of Cardiovascular Electrophysiology, 24,* 132–138.
2. URL [Internet]. Available from: http://www.medtronic.com/for-healthcare-professionals/products-therapies/cardiac-rhythm/ablation-products-for-atrial-fibrillation/arctic-front/index.htm#tab1, Accessed 24th of July 2013.
3. Andrade, J. G., Dubuc, M., Guerra, P. G., Landry, E., Coulombe, N., Leduc, H., Rivard, L., Macle, L., Thibault, B., Talajic, M., Roy, D., & Khairy, P. (2013). Pulmonary vein isolation using a second-generation cryoballoon catheter: a randomized comparison of ablation duration and method of deflation. *Journal of Cardiovascular Electrophysiology, 24,* 692–698.
4. Coulombe, N., Paulin, J., & Su, W. (2013). Improved *in vivo* performance of second-generation cryoballoon for pulmonary vein isolation. *Journal of Cardiovascular Electrophysiology, 24,* 919–925.
5. Fürnkranz, A., Bordignon, S., Schmidt, B., Gunawardene, M., Schulte-Hahn, B., Urban, V., Bode, F., Nowak, B., & Chun, J. K. R. (2013). Improved procedural efficacy of pulmonary vein isolation using the novel second-generation cryoballoon. *Journal of Cardiovascular Electrophysiology, 24,* 492–497.
6. Hussain, S. K., & Ferguson, J. D. (2013). Cool enough-halving pulmonary vein isolation time with the cryoballoon catheter. *Journal of Cardiovascular Electrophysiology, 24,* 699–700.
7. Andrade, J. G., Dubuc, M., Guerra, P. G., Macle, L., Mondésert, B., Rivard, L., Roy, D., Talajic, M., Thibault, B., & Khairy, P. (2012). The biophysics and biomechanics of cryoballoon ablation. *Pacing and Clinical Electrophysiology, 35,* 1162–1168.
8. Available from: http://www.accessdata.fda.gov/scripts/cdrh/cfdocs/cfpma/pma.cfm?id=19003, Accessed 17th of September 2013.
9. Kühne, M., Knecht, S., Altmann, D., Kawel, N., Ammann, P., Schaer, B., Osswald, S., & Sticherling, C. (2013). Phrenic nerve palsy during ablation of atrial fibrillation using a 28-mm cryoballoon catheter: predictors and prevention. *Journal of Interventional Cardiac Electrophysiology, 36,* 47–54.